Design and Optimization Method for a High Power Eddy Current Brake with a Magneto Isotropic Material Structure for the Use in Electrified Heavy Duty Trucks

Christoph Holtmann [1*]

[1]*German Aerospace Centre (DLR)*
Institute of Vehicle Concepts, Alternative Energy Converters
Pfaffenwaldring 38-40, 70569 Stuttgart, Germany (E-mail: christoph.holtmann@dlr.de)

ABSTRACT: In this work, an eddy current brake (ECB) with a magneto isotropic material structure that eliminates the skin effect is shown, which is optimized in this work for an electrified heavy duty truck. Due to the isotropic structure the eddy currents and the heat are distributed almost homogeneously in the material. The material structure consists of steel pins which transfer the magnetic flux from the poles through perforated aluminium sheets. Coolant flows between the aluminium sheets and the number and thickness of the sheets can be selected almost freely, thereby dramatically increasing the surface area in contact with the cooling liquid. The work focuses primarily on the design and optimization method based on a electromagnetic model of the eddy current brake and thermal models for the excitation windings. The electromagnetic model for calculating the torque as a result of the eddy currents is validated with an error of less than 10%. Further, the results of the optimization method show that in emergency braking more than 80% of the braking energy can be converted with the eddy current brake shown here at a power density of approx. 10 kW / kg.

KEY WORDS: eddy current brake, retarder, heavy duty truck, skin effect, isotropic, thermal model, excitation windings

1. Introduction

In electric vehicle applications, the braking technology has changed so that a part of the kinetic energy can be fed back into the battery with the traction machine. However in the case of a emergency braking the required braking power in a car is about 8 times and in commercial vehicle applications about 30 times higher than the drive power rating. This circumstance is the reason that mechanical friction brakes continue to be needed.

In large commercial vehicle applications, retarder technologies have a long history of reducing the wear of the mechanical brakes and reduce maintenance costs. The combination of the electric drive train with a retarder allows to reduce the required size of a mechanical friction brake dramatically. The idea of combining a eddy current brake (ECB) with a mechanical friction brake was already proposed in [1]. However, the power density of retarders, especially of eddy current retarders are much less compared to mechanical friction brakes. The reason for this is the need for a heavy magnetic excitation circuit, while mechanical brakes in addition to the brake disc only need a calliper.

From an electromagnetic point of view, the power density of eddy current brakes in different works has been increased by various measures. One of the most effective measures to increase power density from an electromagnetic viewpoint is to apply a thin layer of highly conductive material to the surface of the active eddy current material, as shown in [2]. However, when this type of eddy current brake is optimized for high speeds, the power density is limited by the thermal behaviour. From a thermal point of view conventional eddy current brakes are comparable to mechanical brakes because the braking power is converted to heat in a solid disc. In further detail both are still comparable, since the skin effect [7] in an ECB let the heat arising in a thin layer on the material surface of the disc as in mechanical friction brakes. In consequence conventional eddy current brakes can never reach the power density of mechanical friction brakes. In order to reduce the possibility of overheating, patent [3] describes a liquid-cooled eddy current brake which can be flooded with water to cool the eddy-current material also from the rotor side. The Disadvantage of this eddy current brake is that the rotor rotates in the water and the torque cannot be controlled quickly. Another possibility is to place small cooling channels near the surface where the eddy currents occur, as shown in [4], but the cooling channels near the surface weaken the primary magnetic field and the torque density decreases.

In this work, an eddy current brake with a magneto-isotropic material structure that reduces the skin effect is shown. The eddy currents and the heat are thus distributed almost homogeneously in the material. The material structure consists of steel pins that transfers the magnetic flux from the poles through perforated aluminium sheets. Coolant flows between the aluminium sheets and the number and thickness of the sheets can be selected almost freely, thereby dramatically increasing the surface area in contact with the cooling liquid.

2. Eddy Current Brake with Magnetoisotropic Structure

Conventional eddy current brakes consist of a homogeneous material that moves at a relative speed v through an inhomogeneous primary magnetic field [5] [6]. The resulting eddy currents lead to a suppression of the field and thus to the phenomenon of the skin effect [7]. The skin effect is primarily the result of the homogeneous material, in which each infinitely small current is coupled to all others through a magnetic circuit with high permeability. The skin effect can be drastically reduced by interrupting the magnetic circuit in the active material in one direction, so that a conductive material can still be penetrated by the primary magnetic field. This can be realized by using pins that only lead the magnetic field in perpendicular to the surface and the pins are surrounded by a conductive material in which the eddy currents occur, as shown in Figure 2and patent [8]. This method is generally not new, since more or less every electrical machine consists of a magnetically conductive material which is surrounded by an electrically conductive material. However, the pin structure enables a new design for the cooling structure. The basic idea to increase the heat-flux in the cooling fluid is to increase the surface of the eddy current material in contact with the fluid. In the eddy current brake with pin structure, the surrounding material can be divided into a number of layers so that the cooling surface is dramatically increased. This method is particularly useful because the eddy current density in each sheet is the same due to the reduction of the skin effect. The setting of the parameters of the material structure can be compared to a free parametrization of the conductivity and permeability of a homogeneous material. The average conductivity of the eddy current material for a given total thickness of the structure can be adjusted by the number of sheets and their thickness, while the permeability can be adjusted by the number of pins and their thickness.

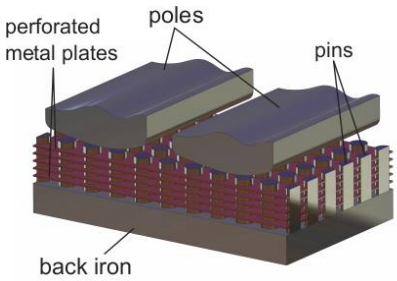

Figure 2: One pole pair of an eddy current brake with magnetoisotropic material structure

In conclusion the advantages of the eddy current brake are:

- reducing the skin effect resulting a more homogenous heat generation
- the possibility of increasing the cooling surface
- free material parametrisation for optimising the torque density and torque characteristics

3. Design and Optimization Process

The eddy current brake is integrated in every motor of an electrified truck with a wheel-specific drive train (see Figure 3) and runs at the same speed as the drive motor in front of the transmission. For the design, it is assumed that the traction motor cannot generate torque in an emergency case. Therefore, the eddy current brake and an additional friction brake must generate the required total braking force shown in Figure 1. Table 1 shows the resulting required brake performance parameter for one wheel of the rear axle, which this work is focused on.

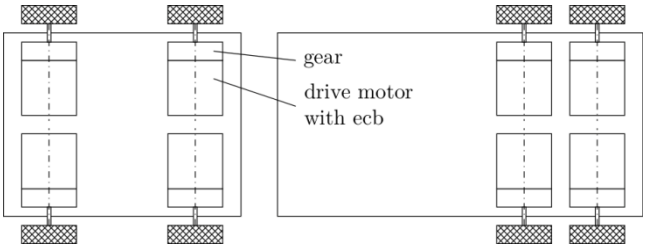

Figure 3: Propulsion concept of the electrified heavy duty truck

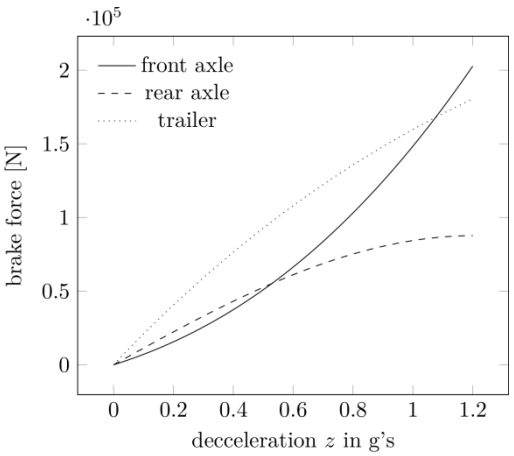

Figure 1: Brake forces of a large heavy truck at the axles

Table 1: Parameter for the reqiered brake performance of one wheel of the rear axle

parameter	symbol	value	unit
Max. velocity	v_{max}	100/3.6	$m\ s^{-1}$
Wheel diameter	d_w	0.9	m
Max. speed drive motor	n_{maxdM}	8000/60	s^{-1}
req. braking torque wheel	M_{reqw}	36000/2	Nm
req. braking torque @ n_{dM}	M_{req}	2600/2	Nm

The aim of the optimization is to find the geometrical parameters of the ECB which reduce the need to use the mechanical brake to a minimum. Because the wear of a mechanical friction brakes is approximatly proportional to the converted braking energy [9], a wear reduction factor is defined with

$$\Delta\varepsilon_w = \frac{E_{ec}}{E_B} = \frac{\int M_{ec}(t) 2\pi n(t)\, dt}{\int M_{req}(t) 2\pi n(t) dt} \quad (1)$$

where E_{ec} is the brake energy converted by the eddy current brake and E_B the total brake energy. The torque of the eddy current

brake M_{ec} is the difference between the requiered torque M_{req} and the torque of the friction brake M_{fric} as illustrated in Figure 4.

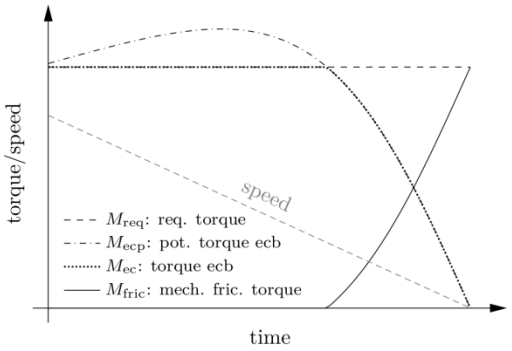

Figure 4: Theoretical torques with linearly decreasing speed over time.

The torque of the ECB at maximum excitation current M_{ecp} can potentially be higher than the requiered torque. In practice, the torque of the eddy current brake is controlled so that it corresponds to the maximum required torque. Since the torque of the friction brake cannot become negative, the following applies

$$\mathrm{M_{fric}} = \frac{1}{2}\left(M_{req} - M_{ecp} + \left|M_{req} - M_{ecp}\right|\right) \tag{2}$$

Hence the torque of the eddy current brake is

$$\mathrm{M_{ec}} = M_{req} - \frac{1}{2}\left(M_{req} - M_{ecp} + \left|M_{req} - M_{ecp}\right|\right). \tag{3}$$

Figure 5 shows the calculation process during optimization. The geometric parameters are fed together with the requirements into a model of the eddy current brake. Since the torque of an ECB primarily depends on the size of the primary magnetic field generated by the excitation current, the maximum permissible excitation current is first calculated in the ECB model using a thermal model of the excitation windings. The maximum excitation current is limited by the allowed winding temperature and or the maximum excitation power.

In parallel, the required cooling surface and thus the required number of sheets in the material structure is determined in a thermal model of the active material in which the eddy currents occur. The overall calculation of the required number of sheets is

$$\mathrm{N_{sh}} = \frac{P_{ecmax}}{A_{sh}\,\dot{q}} \tag{4}$$

where P_{ecmax} is the maximum power generated by eddy currents, A_{sh} the surface area of one sheet and $\dot{q}$ the specific heat flux. When water is used as cooling fluid and the sheets heating up over 100°C at atmospheric pressure the water starts to boil and the specific heat flux reaches values up to 10^6 Wm^{-2} [10]. For safety a value of $\dot{q} = 2 \cdot 10^5$ is used.

At this point the geometrical parameters and the excitation current are fed in a electromagnetic model where the potential torque of the eddy current brake is calculated. Finially the wear reduction $\Delta\varepsilon_w$ gets determined with equation (1) after simulating a type 1 braking cycle.

The optimization algorithm is based on a quadratic interpolation, in which the wear reduction factor is approximated with a quadratic function of the geometric parameters in order to find the optimum iteratively. Since the optimum of a parameter depends on all other parameters, the optimization takes place in nested loops as shown in [11].

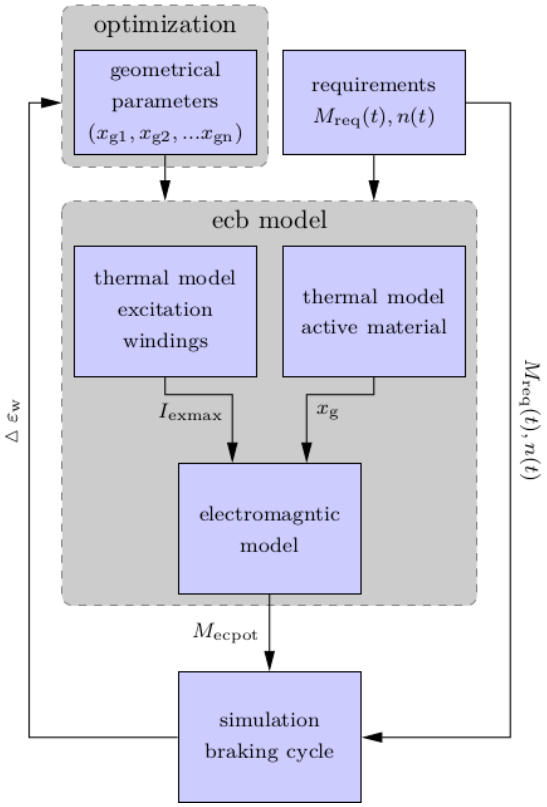

Figure 5: Calculation procedure in the optimization prozess.

4. Modells

The eddy current brake is a double-sided axial flow eddy current brake according to Figure 6 with the effective outside diameter d_o and inside diameter d_i. All models refer to a pole cross-section, which is shown with the detail in Figure 6 at the effective mean diameter.

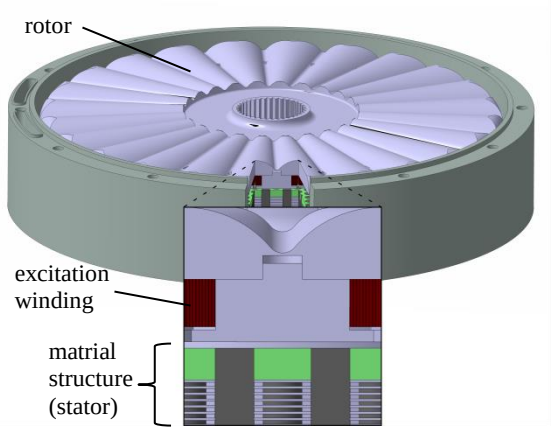

Figure 6: CAD Modell of a double sided axial flux eddy current brake with magnetoisotropic material structure.

4.1. Thermal Model of Excitation Windings

The thermal model of the rotor with excitation windings is required to determine the maximum permissible current density during a Type I braking cycle. In order to minimize the calculation time in the optimization process, the model is made as simple as possible. The model is therefore reduced to a transient 1-d model, which is shown in Figure 7. For simplification, the cross section of the yoke A_y (see Figure 8) and the windings A_w is reduced to the quarter cross section of a cylinder shown in Figure 7. So the heat diffusion equation reduces to

$$\rho \frac{\partial \vartheta}{\partial t} = \frac{1}{r}\frac{\partial}{\partial r}\left(r\lambda \frac{\partial \vartheta}{\partial r}\right) + \dot{q} \tag{5}$$

where ϑ is the temperature, λ the heat conductivity, ρ the density and $\dot{q}$ the volumetric heat generation rate. With the current density j and the electric conductivity $\sigma(\vartheta)$ the heat generation rate in the windings form $r=0$ to $r=r_w$ is

$$\dot{q} = \frac{j^2}{\sigma(\vartheta)} \qquad 0 < r < r_w \tag{6}$$

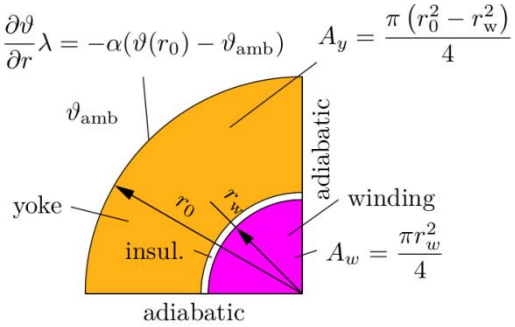

Figure 7: Analytical thermal model of the rotor simplyfied in cylindrical coordinates.

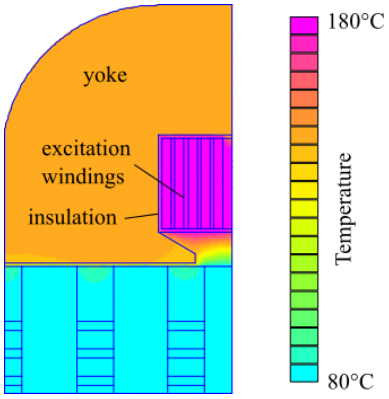

Figure 8: Temperature of the ECB in one half pole cross section as a result of a fem calculation.

The solution of the steady state of equation (5) with the applied current density resulting in the maximum allowable temperature of 180°C is shown in Figure 9. The result is compared to a numerical 2-D-solution that shows a temperature of 177°C for the windings. The 1-D model is therefore precise enough to iteratively calculate the maximum current density.

In each iteration step, the temperature is determined by a transient simulation of a braking cycle with N periods of the duration $t_{bc} = t_a + t_b$, where t_b is the braking time while the windings are loaded with the maximum current density and heat up and t_a is the time of acceleration, in which the windings cool down. If the temperature of the windings is less than permissible, the current density is increased, and if it is higher, it is reduced in the next iteration step.

Figure 10 shows the winding temperature and the excitation power as a function of time as a result of the transient thermal 1-D simulation during a type I braking cycle with 3 periods. As the electric conductivity decreases with increasing temperature, the excitation power also increases during the braking process.

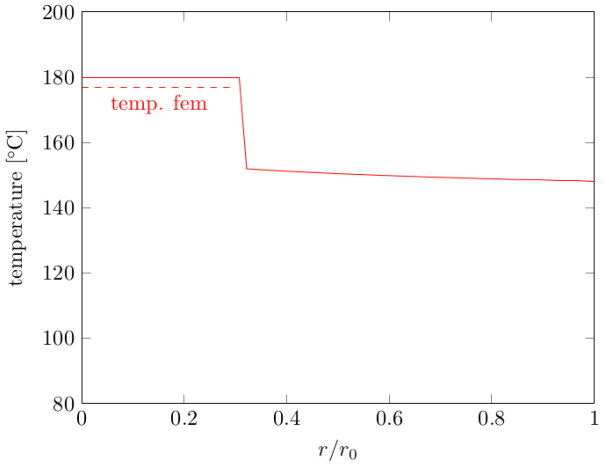

Figure 9: Temperature of the rotor with excitation windings as a result of an analytical 1-d calculation. The dashed line markes the temperature of the windings as a result of the fem calculation with identical input parameters.

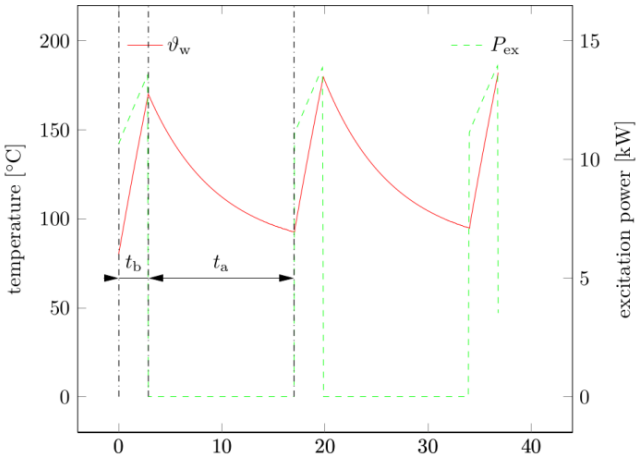

Figure 10: Winding temperature and excitation power over a braking cycle with 3 periods.

4.2. Electromagnetic Model

The main goal of the model [12] is to compute the ECB's torque speed curve for a given geometry and excitation current. The average torque $\bar{M}$ over one revolution at angular speed ω, constant excitation current and constant temperature of an eddy current brake can be determined from the energy balance of the eddy current brake, including the mechanical power $\bar{M}\omega$, the average ohmic losses in the active material as a result of the eddy currents $\bar{P}_{\text{eddy}}$, the average hysteresis losses and the mechanical friction losses $\bar{P}_{\text{fric}}$. In the ECB of this work, the hysteresis losses are only taken into account in the pins and mixed with eddy current losses in the pins to the pin iron losses $\bar{P}_{\text{piron}}$.

$$\bar{M} = \frac{\bar{P}_{eddy} + \bar{P}_{piron} + \bar{P}_{fric}}{\omega} \tag{7}$$

The model is based on the following assumptions and simplifications

- the model is a reluctance-network
- the magnetic circuit is modeled two-dimensionally in a pole cross section at the mean effective radius in order to calculate the mean eddy current across all pin columns in the radial direction.

In order to model the details such as the field repression in the steel pins, the reluctance model contains the results of three sub-models that are not shown in this paper. In the first, the pin model, the complex average relative permeability of a pin is calculated depending on the field strength and the frequency. The second model is used to calculate air reluctances and the third to calculate the electrical resistance of the eddy current path between two pins.

Figure 11 shows the reluctance network with N_{rm} pins in one pole pitch τ_{pm}. The excitation current I_{ex} together with the eddy currents j_{ij} in the eddy current material causes a magnetic flux Φ_{ij} in each pin segment, where i is the pin index in the tangential (movement) direction and j is the index of a pin segment in axial direction.

The reluctance network result in the mesh equation

$$\left(\sum_n R_{\text{m}ijn}\right)\phi_{\text{m}ij} - \sum_n \left(\phi_{\text{m}ijn} R_{\text{m}ijn}\right) = = -\frac{\phi_{\text{m}(i+1)j} - \phi_{\text{m}(i-1)j}}{R_e 2w_{pm}} v + I_{ex}, \tag{8}$$

where $\phi_{\text{m}ij}$ is mesh flux of the mesh ij, R_{ijn} are the path reluctances of one mesh ij to neighboured meshes with the flux $\phi_{\text{m}ijn}$, R_e is the electric resistance of one eddy current path and I_{ex} is the external applied excitation current which only exists in the meshes with excitation windings. The first term on the right represents the eddy currents j_{ij} as a result of the flux change and is the outcome of applying the chain rule to the flux change over time due to the speed of the rotor v at the mean effective radius and the discretization by central difference, where w_{pm} is the distance between two adjacent pins in the direction of movement.

$$\frac{\partial \phi_{\text{m}ij}}{\partial t} = \frac{\partial \phi_{\text{m}ij}}{\partial x}\frac{\partial x}{\partial t} = \frac{\partial \phi_{mij}}{\partial x} v \approx \frac{\phi_{\text{m}\,i+1j} - \phi_{\text{m}i-1,j}}{2w_{\text{pm}}} v \tag{9}$$

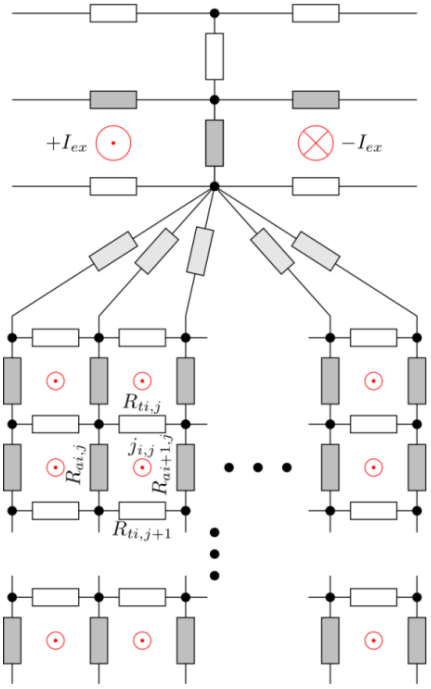

Figure 11: Reluctance network of the eddy current brake. Steel reluctances grey, air reluctances white and airgab reluctance leight grey as they includes the reluctance of the end of the pins.

To validate the electromagnetic model [12], an experimental eddy current brake is constructed including the proposed magnetoisotropic material structure. The torque speed curve of the eddy current brake is measured for different excitation currents as shown in Figure 12. With the 2D reluctance model the torque speed curves can be calculated with an error of less than 10%.

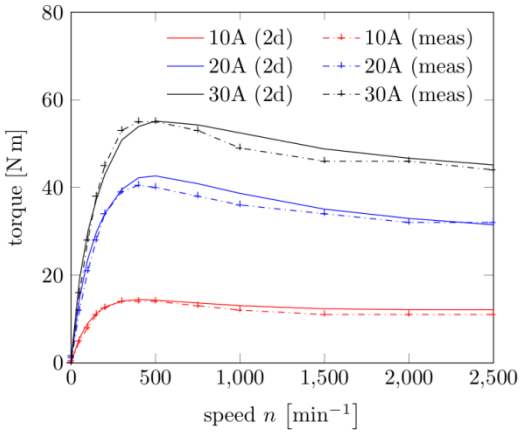

Figure 12: Measured and predicted torque speed curves for different excitation currents.

5. Optimization Results

The optimization is done for different maximum excitation powers because the excitation current has to be fed in the moing rotor at high speeds. For this a brushless rotor power supply is used as proposed in [1]. Within the optimization it turned out that the maximum excitiation power is the limiting factor and not the maximum allowed winding temperature. Figure 13 shows the wear reduction factor for different design points for different allowed excitation powers. From 3.6 kW to 5.1 kW the wear reduction factor increase by about 0.08 per KW and by 0.03 per kW after 5.1 kW. So the design point with the maximum wear reduction factor at 5.1 kW excitation power is shosen for the first prototype construction as shown in Figure 15.

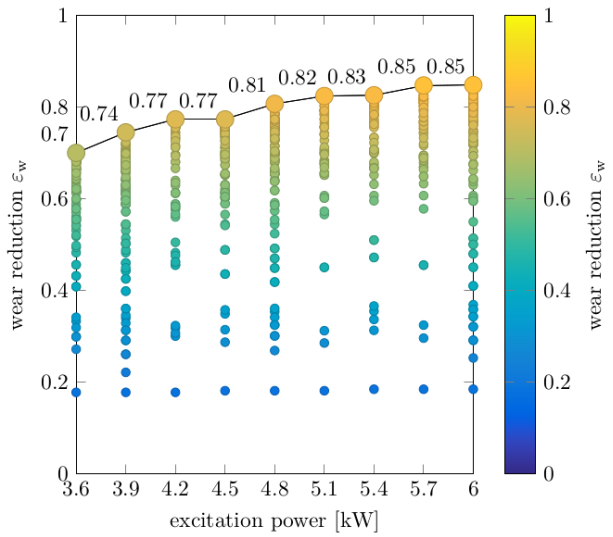

Figure 13: Result of the optimization of the wear reduction for different maximum allowed excitation powers.

The resulting torque over time with linear decresing speed for this design is shown in Figure 14 resulting a wear reduction factor of $\Delta\varepsilon_w = 0.83$ and a power density of 10 kW kg^{-1}.

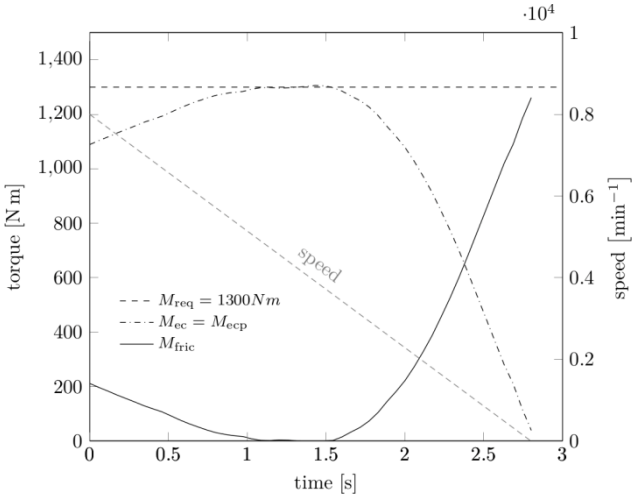

Figure 14: Torques over time at linear decreaing speed for the optimized design of the eddy current brakes.

6. Conclusion and future work

In this work a concept of an eddy current brake was shown that is able to reduce the wear of a breaking system up to 83% during a emergency breaking. The design mehod was shown that also includes a braking test to make shure that the excitation windings do not overheat. Due to the integration of the eddy current brake in the drive unit to a combined propulsion braking unit it is possible to use the cooling circuit of the motor to cool the magnetoisotropic material structure of the eddy current brake.

In the near future a prototype of a combined propulsion braking unit with the eddy current brake proposed in this work as shown in Figure 15 will be testet.

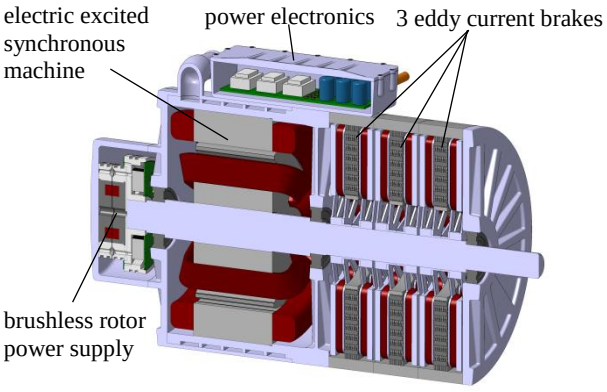

Figure 15: CAD model of a combined propulsion braking unit

The test will also include a further validation of the electromagnetic and thermal models and foremost the wear reduction factor. Further the eddy current brake will be extendet to a hybrid brake that uses the attraction force between rotor and stator to generate a mechanical friction torque at low speeds where the eddy currents are to low to genearate a contact free braking torque. This concept is shown in [1].

References

[1] S. E. Gay, “Contactless magnetic brake for automotive applications,” Ph.D. dissertation, Texas A & M University, 2010.

[2] S. Anwar and R. Stevenson, “Torque characteristics analysis for optimal design of a copper-layered eddy current brake system,” *International Journal of Automotive Technology*, vol. 12, no. 4, pp. 497–502, 2011.

[3] A. Seiwald, “liquid-cooled eddy current brake,” International Patent WO2008/028673Al, Sep. 8, 2008.

[4] E. Flach, “Wirbelstrombremse,” German Patent DE10122985 B4, Aug. 29, 2013.

[5] W. Zimmermann, “Rechnung und Versuch bei der scheibenförmigen Wirbelstrombremse,” *Archiv für Elektrotechnik*, vol. 10, no. 3-4, pp. 133–156, 1921.

[6] W. Smythe, “On eddy currents in a rotating disk,” *Electrical Engineering*, vol. 61, no. 9, pp. 681–684, 1942.

[7] H. A. Wheeler, “Formulas for the skin effect,” *Proceedings of the IRE*, vol. 30, no. 9, pp. 412–424, 1942.

[8] C. Holtmann, “Elektrodynamische Bremse,” German Patent DE102016108646B4, 2019.

[9] E.-C. von Glasner, “Bremssysteme und Bremsverhalten von Nutzfahrzeugen und Zügen,” in *Bremsenhandbuch*. Springer, 2012, pp. 165–197.

[10] S. H. Bomar, “Heat transfer from electrically heated thin metal films to water in pool boiling,” Ph.D. dissertation, Georgia Institute of Technology, 1967.

[11] C. Holtmann, F. Rinderknecht, and H. E. Friedrich, “Simplified model of eddy current brakes and its use for optimization,” in *2015 Tenth International Conference on Ecological Vehicles and Renewable Energies (EVER)*. IEEE, 2015, pp. 1–8.

[12] Holtmann, Christoph, and Andreas Möckel. "2D Reluctance Model of an Eddy Current Brake with a Magneto Isotropic Material Structure." *2020 International Conference on Electrical Machines (ICEM)*. Vol. 1. IEEE, 2020.

[13] J. Veitengruber, “Optimal design of a highly integrated brushless rotor power supply for electrically-excited generators in vehicle-related applications,” in *2015 IEEE Vehicle Power and Propulsion Conference (VPPC)*. IEEE, 2015, pp. 1–7.

[14] C. Holtmann, “Bremsvorrichtung und Fahrzeug,” German Patent DE102018212386A1, Jan. 30, 2020.